

GEOLOGICAL INTERPRETATION OF AERIAL
SPECTROMETRIC AND MAGNETIC SURVEY DATA,
WADI HAMMAD-WADI QENA AREA, EASTERN
DESERT , EGYPT.

Thesis

Submitted in Partial Fulfillment of requirements for the
DEGREE OF MASTER OF SCIENCE

(GEOLOGY)

By

550
M.A

MOHAMMED AHMED EL SADEK

(B . Sc .)

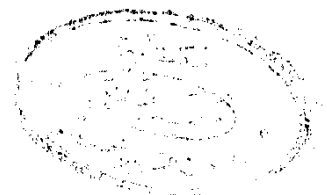
FACULTY OF SCIENCE

AIN SHAMS UNIVERSITY

1993

216

15



ACKNOWLEDGMENTS

The author wishes to express his thanks and gratitude to Dr. Ahmed M. Sabrie, Professor of geophysics, and head of the Geophysics Dept. , Faculty of Science, Ain Shams University, Cairo, Egypt, for his supervision of this study.

The author would like to express his thanks and appreciation to Dr. Ahmed A. Ammar, Professor of applied geophysics, and head of the Exploration Division, Nuclear Materials Authority, Cairo, Egypt, for his sincere guidance, fruitful discussions, supervision and continued help in the interpretation of this study.

The author is especially grateful to Dr. Elsayed M. El Kattan, Assistant professor of applied geophysics, Exploration Division, Nuclear Materials Authority, Cairo, Egypt, for his continuous help, supervision and guidance throughout this study.

The author would like to express his gratitude to Prof. Dr. Nabil M. T. EL Hazeq, President of the Nuclear Materials Authority, Cairo, Egypt.

The author is also grateful to all members of the Exploration Division, Nuclear Materials Authority, Cairo, Egypt. Special thanks are also due to my wife.



CONTENTS

	PAGE
ACKNOWLEDGEMENTS	
CONTENTS	I
LIST OF FIGURES	VI
LIST OF TABLES	XIII
LIST OF PLATES	XVII
CHAPTER I INTRODUCTION.	1
CHAPTER II GEOLOGICAL OUTLINES	5
II.1. GENERAL.	5
II.2. FIELD RELATIONS.	7
II.2.1. Precambrian Basement Rocks.	8
<i>A. Metavolcanics.</i>	8
<i>B. Syntectonic to late tectonic granodiorites.</i>	9
<i>C. Dokhan volcanics.</i>	9
<i>D. Hammamat sediments.</i>	11
<i>E. Younger granites.</i>	13
<i>F. Dykes.</i>	14
II.2.2. Phanerozoic Cover Sediments.	15
<i>A. Nubian formation.</i>	15
<i>B. Quaternary sediments.</i>	15
II.3. STRUCTURES.	16

II.4. MINERALIZATIONS.	17
CHAPTER III AIRBORNE GAMMA-RAY SPECTROMETRIC SURVEY.	19
III.1. GENERAL	19
III.2. INTERACTION OF GAMMA-RAYS WITH MATTER.	24
III.3. ATTENUATION OF GAMMA-RAY FLUX WITH HEIGHT.	25
III.4. AIR ABSORPTION OR ALTITUDE ATTENUATION COEFFICIENTS.	26
III.5. BACKGROUND RADIATION.	27
III.6. STRIPPING RATIOS.	28
III.7. RADIOELEMENTS IN BEDROCK.	29
III.8. SOURCES OF ERROR.	31
III.9. PERFORMANCE OF SURVEY.	33
CHAPTER IV AIRBORNE MAGNETIC SURVEY.	38
IV.1. GENERAL.	38
IV.2. ROCK MAGNETISM.	39
IV.3. MAGNETOMETERS.	40
IV.4. RECORDING SYSTEM.	40
IV.5. FLIGHT DIRECTION.	41
IV.6. LINE SPACING.	41
IV.7. FLIGHT ALTITUDE.	42
IV.8. MAGNETIC PROCESSING.	43
CHAPTER V INTERPRETATION OF AERORADIOMETRIC	45

SURVEY DATA.

V.1. GENERAL.	45
V.2. TECHNIQUES OF STATISTICAL ANALYSIS.	45
V.2.1. The Arithmetic Mean (\bar{X}).	47
V.2.2. The Variance (S^2).	47
V.2.3. The chi-square (χ^2) Test.	48
V.2.4. Bartlett's Test.	49
V.2.5. Analysis of Variance (ANOVA) Test.	50
V.2.6. The (Fischer) F-Test.	51
V.2.7. Studentized t-Test.	52
V.3. RELATION OF AERORADIOMETRIC SURVEY DATA TO REGIONAL GEOLOGY.	53
V.3.1. General.	53
V.3.2. Precambrian Basement Rocks.	55
A. <i>Metavolcanics.</i>	55
B. <i>Syntectonic to late tectonic granodiorites.</i>	59
C. <i>Dokhan volcanics.</i>	63
D. <i>Hammamat sediments.</i>	68
E. <i>Younger granites.</i>	70
V.3.3. Phanerozoic Cover Sediments.	85
A. <i>Nubian formation.</i>	85
B. <i>Quaternary sediments.</i>	91
V.4. Aeroradioactivity Characteristics of the IRL Units.	95

CHAPTER VI THE DISTRIBUTION OF RADIOELEMENTS IN G. EL GLUF BIOTITE GRANITE, AS A GUIDE TO THE RECOGNITION OF ANOMOLOUSLY RADIOACTIVE ZONES.	101
VI.1. GENERAL.	101
VI.2. METHODS OF ANALYSIS.	103
VI.3. EFFECT OF TOPOGRAPHY, GEOLOGICAL FORMATION AND STRUCTURES ON RADIOMETRIC ANOMALY OCCURRENCE.	108
VI.4. GEOLOGICAL SIGNIFICANCE OF THE GAMMA - RAY SPECTROMETRIC SURVEY DATA.	109
VI.5. RADIOMETRIC ANOMALY AND TECTONIC TREND RELATIONSHIP.	124
VI.6. CONCLUSIONS.	127
CHAPTER VII INTERPRETATION OF AEROMAGNETIC SURVEY DATA.	129
VII.1. GENERAL.	129
VII.2. TECHNIQUES OF INTERPRETATION OF AERO- MAGNETIC DATA.	133
VII.2.1. Reduction-to-Pole.	133
VII.2.2. Separation of Magnetic Anomalies (Filtering).	135
<i>A. Empirical grids-running means method.</i>	136
<i>B. Fast Fourier Transform "FFT" in the frequency domain.</i>	137
VII.2.3. Trend Analysis.	141
<i>A. General.</i>	141
<i>B. Rose diagrams.</i>	143
<i>C. The overlap method.</i>	143

VII.2.4. Depth Determination.	146
<i>A. General.</i>	146
<i>B. Half-width method.</i>	147
<i>C. Straight slope method.</i>	148
<i>D. Peters's method.</i>	148
<i>E. Smellie's method.</i>	149
<i>F. Fast Fourier Transform (FFT) technique.</i>	151
VII.3. CORRELATION OF AEROMAGNETIC SURVEY DATA TO REGIONAL GEOLOGY.	154
VII.3.1. Discussion of the Results of Trend Analysis	154
<i>A. North-south (east-african) trend.</i>	154
<i>B. Northwest (erythrean) trend.</i>	155
<i>C. Northeast (australitic) trend.</i>	157
<i>D. North northeast (Aqaba) trend .</i>	158
<i>E. East-west (tethyan or mediterranean) trend.</i>	159
VII.3.2. Discussion of the Results of Depth Estimation.	169
VII.3.3. Basement Tectonic Map.	178
SUMMARY AND CONCLUSIONS.	181
REFERENCES.	187
ARABIC SUMMARY.	

LIST OF FIGURES

Figure No.		Page
1	Map of Egypt showing the location of Wadi Hammad - Wadi Qena Area, North Eastern Desert, Egypt .	2
2	A typical airborne gamma ray spectrum showing the gamma ray peaks of the three radioelements, along with the energy windows used to detect them at 120 meters above the ground.	21
3	Interaction of gamma rays with materials.	25
4	Variation in average K,U. and Th contents with increasing Si content, from ultrabasic to acid igneous rocks.	30
5	Variation in average radioelement ratios with increasing Si content, from ultrabasic to acid igneous rocks	30
6	Index map showing the airborne spectrometric and magnetic surveys conducted by Aero Service, 1984, in relation to Wadi Hammad - Wadi Qena area, North Eastern Desert, Egypt.	34
7	Frequency distribution histograms of the aeroradioactivity data with fitted theoretical curves, Metavolcanics (MV), Wadi Hammad-Wadi Qena area, North Eastern Desert, Egypt.	57
8	Frequency distribution histograms of the aeroradioactivity data with fitted theoretical curves, Granodiorites (GD), Wadi Hammad-Wadi Qena area, North Eastern Desert, Egypt.	61
9	Frequency distribution histograms of the aeroradioactivity data with fitted theoretical curves, Dokhan Volcanics (DV), Wadi Hammad-Wadi Qena area, North Eastern Desert, Egypt	66

10	Frequency distribution histogram of the aeroradioactivity data with fitted theoretical curve, Hammamat Sediments (HS), Wadi Hammad - Wadi Qena area, North Eastern Desert, Egypt.	69
11	Frequency distribution histogram of the aeroradioactivity data with fitted theoretical curve, the first Younger Granite pluton (YG-1), Wadi Hammad - Wadi Qena area, North Eastern Desert, Egypt.	71
12	Frequency distribution histograms of the aeroradioactivity data with fitted theoretical curves, the second Younger Granite pluton (YG-2) and its subdivisions (YG-2a and YG-2b), Wadi Hammad-Wadi Qena area, North Eastern Desert, Egypt.	73
13	Frequency distribution histograms of the aeroradioactivity data with fitted theoretical curves, the third Younger Granite (YG-3) pluton, and its subdivisions (YG - 3a, YG - 3b and YG - 3c), Wadi Hammad-Wadi Qena area, North Eastern Desert, Egypt.	75
14	Frequency distribution histograms of the aeroradioactivity data with fitted theoretical curves, the fourth Younger Granite pluton (YG-4) and its subdivisions (YG - 4a and YG - 4b), Wadi Hammad-Wadi Qena area, North Eastern Desert, Egypt.	77
15	Frequency distribution histogram of the aeroradioactivity data with fitted theoretical curve, of the fifth Younger Granite pluton (YG-5), Wadi Hammad - Wadi Qena area, North Eastern Desert, Egypt.	79

16	Frequency distribution histograms of the aeroradioactivity data with fitted theoretical curves, Nubian Formation (NF) and its subdivisions (NF - 1 and NF - 2), Wadi Hammad-Wadi Qena area, North Eastern Desert, Egypt.	86
17	Frequency distribution histograms of the aeroradioactivity data with fitted theoretical curves, Nubian Formation (NF) and its subdivisions (NF-3 and NF-4), Wadi Hammad - Wadi Qena area, North Eastern Desert, Egypt.	88
18	Frequency distribution histograms of the aeroradioactivity data with fitted theoretical curves, Quaternary Sediments (QS), Wadi Hammad- Wadi Qena area, North Eastern Desert, Egypt.	92
19	Relation between the types and the relative ages of the various rock groups with their grand mean and range of arithmetic means, Wadi Hammad - Wadi Qena area, North Eastern Desert, Egypt.	96
20	Detailed graphs showing the variation of the arithmetic mean (\bar{X}) and back-ground of aeroradioactivity ($X \pm 3S$) in Ur, of the different interpreted radio-litho (IRL) units, arranged according to growing radioactivity of the various rock groups, Wadi Hammad - Wadi Qena area, North Eastern Desert, Egypt.	97
21	Topographic Map of the El Gluf Area, North Eastern Desert, Egypt.	102
22	Geological Map of the El Gluf Area, North Eastern Desert, Egypt.	104
23	Total Count Airborne Radioactivity Map of the El Gluf Area, North Eastern Desert, Egypt.	104

24	Potassium Airborne Spectrometric Map of the El Gluf Area, North Eastern Desert, Egypt.	105
25	Equivalent Uranium Airborne Spectrometric Map of the El Gluf Area, North Eastern Desert, Egypt.	105
26	Equivalent Thorium Airborne Spectrometric Map of the El Gluf Area, North Eastern Desert, Egypt.	106
27	Equivalent Uranium / Equivalent Thorium Ratio Map of the El Gluf Area, North Eastern Desert, Egypt.	106
28	Equivalent Uranium/Potassium Ratio Map of the El Gluf Area, North Eastern Desert, Egypt.	107
29	Equivalent Thorium/Potassium Ratio Map of the El Gluf Area, North Eastern Desert, Egypt.	107
30	Frequency Histogram with Fitted Theoretical Curves for the Total Count Radioactivity, and eTh/k Ratio of the: a- El Gluf Biotite Granite. b- Two subunits (B.G.S.I & B.G.S.II), of El-Gluf Biotite Granite.	112
31	Standard Deviation T.C Anomaly Map of the El Gluf Area, North Eastern Desert, Egypt.	114
32	Standard Deviation K Anomaly Map of the El Gluf Area, North Eastern Desert, Egypt..	114
33	Standard Deviation eU Anomaly Map of the El Gluf Area, North Eastern Desert, Egypt.	115

34	Standard Deviation eTh Anomaly Map of the El Gluf Area, North Eastern Desert, Egypt.	115
35	Standard Deviation eU/eTh Anomaly Map of the El Gluf Area, North Eastern Desert, Egypt.	116
36	Standard Deviation eU/K Anomaly Map of the El Gluf Area, North Eastern Desert, Egypt.	116
37	Standard Deviation eTh/K Anomaly Map of the El Gluf Area, North Eastern Desert, Egypt.	117
38	Interpreted Spectrometric Anomalies and tectonic Trends as Inferred From Different Maps.	117
39	Airborne Gamma-ray spectrometric Profiles over Uranium Anomalies Numbers (1&2), El Gluf Area, North Eastern Desert, Egypt.	118
40	Airborne Gamma-ray spectrometric Profiles over Thorium Anomalies Numbers (1&2), El Gluf Area, North Eastern Desert, Egypt.	119
41	Airborne Gamma-ray spectrometric Profiles over Uranium and Thorium Anomalies Numbers (1&2), El Gluf Area, North Eastern Desert, Egypt.	120
42	Airborne Gamma-ray spectrometric Profiles over Uranium and Thorium Anomalies Number (3), El Gluf Area, North Eastern Desert, Egypt	121
43	Rose Diagrams showing the Relative Frequency Distributions in Percent, EL Gluf Area, North Eastern Desert, Egypt.	126

44	Approximate determination of residual from values sampled on a square grid. Residual around center point is obtained by averaging eight potential field readings and subtracting the central value from the average. Average approximates the potential field along dotted circle.	136
45	Interface determination using local Power Spectrum of the aeromagnetic data, Wadi Hammad-Wadi Qena Area, North Easter Desert, Egypt.	140
46	Depth Determination Methods.	153
47	Rose diagrams for R.T.P. magnetic- and total- count radiometric-trends, Wadi Hammad- Wadi Qena area, North Eastern Desert, Egypt.	160
48	Rose diagrams for regional and residual R.T.P. magnetic-component trends (depth level 1.0 km), Wadi Hammad-Wadi Qena area, North Eastern Desert, Egypt.	161
49	Rose diagrams for regional and residual R.T.P. , magnetic-component trends(depth level 3.0 km), Wadi Hammad-Wadi Qena area, North Eastern Desert, Egypt.	162
50)	Rose diagrams for faults as traced from the geological map and courses of main wadis trends, Wadi Hammad-Wadi Qena area, North Eastern Desert, Egypt.	163
51	Frequency distribution curves of the statistically-analysed of R.T.P. and T.C. radiometric trends, Wadi Hammad-Wadi Qena area, North Eastern Desert, Egypt.	164

52	Frequency distribution curves of the statistically-analysed regional and residual R.T.P. magnetic-component trends, Wadi Hammad-Wadi Qena area, North Eastern Desert, Egypt.	165
53	Frequency distribution curves of the statistically-analysed regional and residual R.T.P. magnetic-component trends, Wadi Hammad - Wadi Qena area, North Eastern Desert, Egypt.	166
54	Frequency distribution curves of the statistically-analysed courses of main wadis as traced from the geological map, Wadi Hammad - Wadi Qena area, North Eastern Desert, Egypt.	167
55	The profiles along which the depths to the causative bodies were determined (their serial No./depth, in m), R.T.P. aeromagnetic map, Wadi Hammad-Wadi Qena area, North Eastern Desert, Egypt.	170
56	The profiles along which the depths to the causative bodies were determined (their serial No./depth, in m), R.T.P. Regional magnetic-component map, Wadi Hammad-Wadi Qena area, North Eastern Desert, Egypt.	171
57	The profiles along which the depths to the causative bodies were determined (their serial No./depth, in m), R.T.P. Residual magnetic component map, Wadi Hammad-Wadi Qena area, North Eastern Desert, Egypt.	172